Bacterial and Archaeal Communities in Recycling Effluents from a Bauxite Flotation Plant

Xinxing LIU[1,2], Yong-Hong WU[1, 2], Xi Liu[3], Han-yan Wu[1, 2], Jianping XIE[1,2], Guohua Wang[4], Guan-zhou QIU[1,2], Qiang HUO[1,2*]

1. School of Minerals Processing and Bioengineering, Central South University, Changsha Hunan, China

2. Key Laboratory of Biohydrometallurgy, Ministry of Education, Central South University, Changsha Hunan, China

3. Zhengzhou Non-ferrous Metals Research Institute Co. Ltd of CHALCO, Zhengzhou Henan, China

4. Hunan Province Key Laboratory of Pollution Control and Resources Reuse Technology, University of South China, Hengyang Hunan, China

*Corresponding author

E-mail: hhhuosun@163.com(QH)

Abstract: Recycling effluent has become a bottleneck and an environmental risk associated with the regular production of bauxite via flotation and the sustainable development of the aluminum industry in China. To find a practical direction for biotreatment, the bacterial and archaeal communities in recycling effluents containing concentrate and tailings from bauxite flotation plants were investigated by a metagenomic sequencing method in association with the evaluated geochemical properties. The results showed that *Paracoccus, Desulfomicrobium, Exiguobacterium, Tindallia, Ercella* and *Anoxynatronum* were the primary bacterial genera and *Methanothrix, Methanobacterium, Nitrososphaera* and *Methanosarcina* were the dominant archaeal genera. Upon combining the microbial diversity and the geochemical properties of the two sample types, the microbial community containing *Desulfomicrobium, Paracoccus, Tindallia, Methanobacterium, Methanothrix* and *Nitrososphaera* was better adapted to the biodegradation of flotation collectors, and the microbial community consisting of *Paracoccus, Exiguobacterium, Methanothrix* and *Methanobacterium* was more efficient at hydrolyzed polyacrylamide (HPAM) biodegradation. In addition, a large proportion of unclassified OTUs has indicated that recycling effluent is a worthy resource for isolating new strains from the Firmicutes phylum.

1 Introduction

China has been the world's leading producer of metallurgical-grade alumina over the last 16 years(1). The operational yield of the Chinese alumina industry in 2017 exceeded 69 million tons, with a year-on-year growth of 13.32%, which resulted in the rapid depletion of high A/S (mass ratio of alumina to silica) bauxite as well as a great challenge to Chinese bauxite resources(2). Bauxite desilication by flotation,

which could be used for low A/S bauxite that is found in large reserves in China, became an important technical method for the sustainable development of the aluminum industry in China(3, 4)

A large amount of water is needed for the bauxite desilication process, and a large quantity of water can be saved by water recycling through flocculation and the rapid settlement of the pulp(5). However, the production index becomes worse with the increased circulation time of the circulating water; the periodic replacement of circulating water was the primary method for solving this problem in bauxite flotation plants, resulting in a problem of recycling effluents. These recycling effluents contained high concentrations of ions and the residues of beneficiation reagents, such as collectors and flocculants(6, 7). The periodic discharge of recycling effluents would have potential environmental risks, but little study has been devoted to this approach. However, with the rapid economic growth and social development in China, the associated problems of water contamination and shortages of water resources have become serious bottlenecks that challenge and limit sustainable development at the regional as well as national levels(8, 9). Finding an efficient and safe method for treating the recycling effluents, such as biological methods, is an urgent task.

Because of the importance of bauxite desilication by flotation for the alumina industry of China and with the increased use of water resources, the microbial communities in the recycling effluents from desilication processing were revealed and linked with the chemical and geographical conditions to create effective advice for the prevention and treatment of these problems. The compositions, diversity and

dynamics of the given microorganisms may interfere in the efficiency and stability of wastewater treatment plants(10). Therefore, studies about the microbial community in these systems have been focused on the functions and performance of wastewater treatment(11). In this study, recycling effluents from the desilication process were collected before being discharged at the bauxite flotation plant in Henan province, and the community structures were assayed using 16S rRNA genes by high-throughput sequencing method.

2 Materials and methods

2.1 Site description and sample collection

Samples of recycling effluent were collected from the bauxite flotation plant located in Henan province. Recycling effluents of concentrates and tailings were collected from a circulating cistern (Fig 1), and they were named HNC and HNT, respectively.

Fig 1 Flow chart of desilication process and sample collection

Water samples were collected in July of 2018. Approximately 25 L of recycling effluent from each circulating cistern was collected, and the temperature and pH of each sample were detected at the same time. The samples were then filtered through a 0.22 μm hyperfiltration membrane with a vacuum pump. The sediments on the membranes were then immediately transferred to a tube and stored at -20℃ for further molecular analysis. The filtered water samples were sent for chemical analysis.

2.2 Geochemical analysis

We measured the concentrations of 28 elements, including Al, As, Ca, Cr, Cu, Fe,

K, Mn, Na, Pd, Zn and other elements, by Inductively Coupled Plasma Mass Spectroscopy (ICP-MS, G8403A, Japan).

2.3 DNA extraction, PCR and sequencing

The DNA in the water samples was extracted from 200 mg of sediment with an E.Z.N.A. Soil DNA Kit (OMEGA, USA). The DNA integrity was detected by agarose gel electrophoresis. Accurate quantitative control of the genomic DNA added to the PCR reaction system was achieved after the determination of the genomic DNA with a Qubit 3.0 DNA detection kit.

The V3-V4 region(12)of the 16S rRNA genes was amplified with the primer pair 341F (5′ -CCCTACACGACGCTCTTCCGATCTG (barcode) CCTACGGGNGGC WGCAGA-3′) and 806R (5′ -GACTGGAGTTCCTTGGCACCCGAGAATTCCAGA CTACHVGGGTATCTAATCC-3′) combined with the universal primers on the MiSeq sequencing platform.

The PCR reactions of the first round had a total volume of 30 µl, which contained 10-20 ng of genomic DNA, 15 µl of 2×Taq master Mix, 1 µl of Bar-PCR primer F (10 µM), 1 µl of primer R (10 µM), and the remaining volume of H_2O. The cycling conditions of the first round were 94℃ for 3 min, 5 cycles of 94℃ for 30 s, 45℃ for 20 s, and 65℃ for 30 s, 20 cycles of 94℃ for 20 s, 55℃ for 20 s, and 72℃ for 30 s, and a final extension at 72℃ for 5 min. The PCR reactions of the second round had a total volume of 30 µl, and they contained 20 ng of genomic DNA, 15 µl of 2×Taq master Mix, 1 µl of primer F (10 µM), 1 µl of primer R (10 µM), and the remaining

105 volume of H_2O. The cycling conditions of the second round were 95℃ for 3 min, 5
106 cycles of 94℃ for 20 s, 55℃ for 20 s, and 72℃ for 30 s, and a final extension at 72℃
107 for 5 min.

108 The PCR products were purified by Agencourt AMPure XP (Beckman, USA) and
109 quantified accurately by Qubit 3.0 DNA detection kit. The PCR products of each
110 sample were mixed to a final concentration of 20 pmol and then sequenced with a
111 MiSeq benchtop sequencer (Illumina, San Diego, USA) for 2×300 bp paired-ends
112 sequencing.

113 **2.4 Sequence data processing and statistical analysis**

114 The sequenced reads with perfect matches to barcodes were split into sample
115 libraries, and the chimeras were high-quality trimmed using Usearch. The OTUs were
116 classified at a 97% similarity level and rarefaction analyses were conducted using
117 Mothur(13). The curves from the rarefaction analysis and rank abundance analysis
118 were marked using the originally detected OTUs from R Project 3.2.

119 The sequences were first filtered through a BLAST search against the RDP
120 database(14), with a common confidence threshold of 80–90%, and the satisfactory
121 sequences were phylogenetically assigned to taxonomic classifications via an RDP
122 naïve Bayesian classifier and Bergey's taxonomy at a 0.03 distance(15). A
123 dendrogram was constructed with data derived from a hierarchical cluster analysis of
124 the beta diversity distance matrix and an unweighted pair group method with
125 arithmetic mean (UPGMA) cluster analysis(16). Bray-Curtis ordination was used to
126 calculate the distance between samples. A phylogenetic tree was constructed with

Python software and functional gene compositions were calculated with PICRUSt 1.0.0 software(17). All the other analyses were performed in R 3.2 with the vegan packages v. 2.0-10.

3 Results and discussion

3.1 Geochemical properties of samples

The plant from which the samples were collected is located in Guanyinsi village, Henan province, China. The two samples were collected outdoors, from the exposed cisterns, and the colors of the two samples were light yellow with some suspended substances. The temperature of them both was approximately 31℃, and the pH values were 9.37 and 9.28 for the HNC and HNT samples, respectively. The detectable ion concentrations are listed in Table 1, and they showed similar concentrations in the two samples. The samples contained a very high level of Na from the addition of $NaCO_3$ during bauxite flotation processing. The concentrations of Al, K and Ca were at a relatively higher level. In addition, the concentrations of Mg, Fe, Zn, Mo and Ba were at a relatively lower level. Some ions, such as Ti, As, Pb, Sb, B, Mn, and Se, showed very low concentrations, while some ions, such as Cu, Ni, Cd, Ag and others, were not detected. The organics in the samples were the residuals of collectors (such as hydroximic acid, oleic oil and others) and flocculants (primarily HPAM).

In all, the two samples were both taken from the bauxite flotation process. They had similar ion concentrations, pH values, temperatures and flocculant concentrations, but they had different concentrations of collectors for the

149 chemical adsorption on concentrate and no effect on the tailings.

150 **Table 1** Geochemical properties of the water samples (mg/L)

Sample	**B**	**Na**	**Mg**	**Al**	**K**	**Ca**	**Mn**	**Fe**	**Zn**	**Ba**
HNC	0.17	1410.96	1.96	6.27	13.89	54.88	0.05	1.46	1.87	1.09
HNT	0.15	1237.35	1.17	5.75	21.70	39.92	0.03	1.69	1.43	0.96
Sample	**Ti**	**As**	**Se**	**Mo**	**Pb**	**Sb**	F^-	NO_3^-	SO_4^-	Cl^-
HNC	0.11	0.01	0.01	0.78	0.01	0.01	6.84	5.17	93.21	121.89
HNT	0.10	0.01	0.01	0.71	0.01	0.01	5.33	1.36	69.15	94.92

151

152 **3.2 Analyses of OTUs**

153 Both sequencing data sets were separated from one another to investigate the core
154 microbiome in recycling effluents of the concentrate and tailings. Furthermore, a
155 differentiation between bacteria and archaea was made to avoid the loss of the
156 archaeal OTUs due to their low sequence reads. More than 35000 high-quality
157 sequences with at least 1600 OTUs for bacteria as well as more than 27000
158 high-quality sequences with at least 320 OTUs for archaea were used for the
159 microbial community composition analysis of the two samples after filtering out the
160 chimeras. The asymptotic level of the Shannon rarefaction curves, at a 97% similarity
161 level, suggested that the number of OTUs were sufficient for this study (Fig 2). The
162 Shannon diversity index of bacterial communities was significantly higher than that of
163 the archaeal communities, which suggested that the bacterial communities were more
164 varied.

Fig 2 Curves from the Shannon rarefaction analysis (a-bacteria, b-archaea)

Rank-abundance curves are used to interpret two aspects of sample diversity, namely the richness and evenness of the species in the sample. Fig 3 shows that the samples had low diversity index for the narrow change along the lateral axis while the two sites had a low degree of uniformity for both archaeal and bacterial compositions because of the steep shapes of the curves. The rarefaction curves combined with the rank abundance curves suggested that the work was able to reveal the real microbial community compositions of the samples.

Fig 3 Rank abundance curves based on OTU ranks (a-bacteria, b-archaea)

A Venn diagram could reflect the similarity and overlap of the OTU composition between samples visually (Fig 4). The samples in this study had low similarity rates in both archaeal and bacteria communities at the OTU level. The bacterial OTUs were more abundant than archaeal OTUs in the two samples, and the microbial composition of the HNC were more abundant than that of the HNT. For both the archaeal and bacterial communities, the common OTUs both detected in the two samples were at a low level for each total OTU number, at 4.09% and 2.57%, respectively. That finding revealed the significant diversity between the HNC and HNT samples that might be caused by the different properties of concentrate and tailings, although both of them were involved in the water cycle of the bauxite flotation process.

Fig 4 Similarity and overlap analysis of OTUs by Venn diagram (a-bacteria, b-archaea)

3.3 Analyses of microbial communities

To identify effective biological methods for the prevention and treatment of the recycling effluents problem, it is vital to comprehensively understand the involved microbial communities in terms of taxonomic compositions, similarity and diversity. A taxonomic composition analysis is one of the most frequently used bioinformatics analyses for microbial communities(18).

(1) Bacterial communities

As illustrated in Fig 5, the dominant bacterial genus was unclassified in the two samples accounting for 38.47% and 45.75% for HNC and HNT, respectively. Interestingly, almost all of the unclassified OTUs fell into the Firmicutes phylum, which suggested a new source for seeking new species in the Firmicutes phylum. For the HNC sample, with the exception of the unclassified bacterial genus, *Desulfomicrobium, Paracoccus* and *Tindallia* were the top three predominant genera, accounting for 29.62%, 10.17% and 8.01%, respectively, followed by *Exiguobacterium, Dethiosulfatibacter, Nitrincola, Anoxynatronum* and *Ercella* with a proportion over 1%. For the HNT sample, except for the unclassified bacterial genus, *Paracoccus* and *Exiguobacterium* were the top two predominant genera, accounting for 21.34% and 17.99%, respectively, followed by *Ercella, Tindallia, Pirellula, Anoxynatronum* and *Ercella,* with a proportion between 1% to 3%.

Fig 5 Taxonomic distribution of bacterial OTU abundance at the phylum level

According to the taxonomic comparison results, the dominant species were selected and the evolutionary relationships and abundance differences in the dominant

209 microorganisms in the sequenced environmental samples were understood from the
210 phylogenetic system (Fig 6). According to the phylogenetic analysis, 99.03% of the
211 bacterial OTUs fell into the following six phylogenetic divisions: Proteobacteria,
212 Firmicutes, Synergistetes, Planctomycetes, Actinobacteria and Acidobacteria.
213 Proteobacteria and Firmicutes were the dominant phyla while the others contributed
214 little to the bacterial community structures.

215 Within the Proteobacteria phylum, which accounted for 35.44% of the bacterial
216 communities, *Paracoccus* belonged to Alphaproteobacteria (mostly found in HNC)
217 and *Dethiosulfatibacter* belonged to Desulfomicrobium (mostly found in HNT) were
218 the major genera. Firmicutes accounted for 59.36% of all the OTUs, but more than
219 half of that OTUs were classified into unknown genera, and 10.17% of all the OTUs
220 fell into the *Exiguobacterium* genus while 5.16% fell into *Tindallia*.

221 **Fig 6 Phylogenetic compositions and community structures of bacteria**

222 *Paracoccus* was found in both samples and played an important role in the
223 bacterial community structures. HPAM, hydroximic acid and oleic oil were the
224 primary organic pollutants in recycling effluents, and the *Paracoccus* genus emerged
225 as a versatile species for the bioremediation of various recalcitrant pollutants, such as
226 pyridine(19), dimethylformamide(20), N-methylpyrrolidone(21), and others.
227 *Paracoccus* was also reported to not only reduce nitrate under an aerobic atmosphere
228 but also to convert ammonium to nitrogen gas via hydroxylamine, nitrite, nitrate and
229 nitrous oxide, which indicated that another nitrogen removal pathway immediately
230 accessible via hydroxylamine without any accumulation of nitrate and nitrite could be

231 responsible for this phenomenon(22). Hydroxylamine from organic pollutants and
232 nitrate from recycling effluents were the primary nitrogen source for microbial growth
233 as well as biodegradation actions.

234 Although several OTUs were detected in the HNT sample, *Desulfomicrobium*
235 was in the majority in the HNC. *Desulfomicrobium* is gram-negative and is commonly
236 found in aquatic environments with high levels of organic matter as well as in sewage
237 sludge as a major community member of extreme oligotrophic habitats(11). Reports
238 revealed the good bioremediation potential of the reductive process performed by
239 *Desulfomicrobium*, and the degradation pathway was that sulfate and other oxidized
240 sulfur compounds serve as terminal electron acceptors and are reduced to H_2S(23).
241 The two samples in this study had similar sulfate concentrations as well as
242 temperature and pH, and the diversity in *Desulfomicrobium* between two samples
243 might be due to that residue of hydroximic acid and oleic oil mostly in concentrate
244 pulp while little of that was associated with tailing pulp for collectors, which were
245 compatible with concentrate(24).

246 Contrary to the distribution of *Desulfomicrobium,* there was little
247 *Exiguobacterium* in the HNC but quite a lot in the HNT. The genus *Exiguobacterium*,
248 which belongs to the Bacilli class, is characterized by the following features: the cells
249 are gram-positive, non-endospore-forming, facultatively anaerobic and
250 oxidase-negative (25). *Exiguobacterium* has been reported to promote plant growth
251 and the degradation of environmental pollutants, to be halotolerant(26, 27) and to be
252 able to produce highly effective proteolytic enzymes(28). The HNT sample had a pH

253 value of approximately 9.28, which provided an environment for the bacteria
254 belonging to the *Exiguobacterium* genus to show their applicability to the biological
255 neutralization of alkaline wastewater(25). The HNC also had a pH value of 9.37 but
256 little *Exiguobacterium*, perhaps because of the inhibition of carbon sources (such as
257 hydroximic acid and oleic oil) and the competition from *Desulfomicrobium*.

258 *Tindallia, Anoxynatronum* and *Ercella* were all detected in the two samples as
259 auxiliary members, and they were all reported to be alkaliphilic and good for potential
260 use in treating alkaline wastewater(29-31).

261 (2) Archaeal communities

262 Archaea, which were originally found in extreme environments, were known to
263 be ubiquitous and crucial partners in numerous microbiomes, either in environmental
264 settings or associated with holobionts(32), and they were no exception in this research.
265 Fig 7 reveals that *Methanobacterium* and *Methanothrix* were the dominant archaeal
266 genera in the two samples, accounting for 46.67% and 30.24%, 75.13% and 19.99%
267 for HNC and HNT, respectively. *Nitrososphaera* was also abundant in HNC, with a
268 proportion of 18.62%, while it contributed only 4.17% to HNT. *Methanosarcina* was
269 found in both samples and accounted for a low proportion of the total.

270 **Fig 7** Taxonomic distribution of archaeal OTU abundance at the phylum level

271 According to the phylogenetic analyses (Fig 8), almost all of the archaeal OTUs
272 fell into the three archaeal phyla Euryarchaeota, Thaumarchaeota and Planctomycetes.
273 Euryarchaeota was dominant and Planctomycetes was seldom identified.
274 Euryarchaeota contains methane-forming, extremely halophilic, sulfate-reducing, and

275 extremely thermophilic sulfur-metabolizing species(33). Although there was a similar
276 distribution in the two samples at the phylum level, *Methanobacterium* was more
277 abundant in the HNC sample and *Methanothrix* was ascendant in the HNT at the
278 genus level under the Euryarchaeota phylum.

279 **Fig 8 Phylogenetic compositions and community structures of archaea**

280 *Methanothrix*, a genus of Methanosarcinales that are typical acetoclastic
281 methanogenic archaea(34), made up more than half of all the OTUs, while
282 *Methanobacterium*, a genus of Methanobacteriales that could reduce CO using
283 molecular hydrogen (hydrogenotrophic) and produce methane(35), accounted for
284 approximately one third of all the OTUs. These two primary genera belong to the
285 methanogenic archaea and made up more than 85% of the archaeal communities. The
286 methanogens were the initially and most widely recognized archaea, and they were
287 considered to play a prominent role in the degradation of complex organic compounds
288 by a consortia of anaerobic microorganisms. The methanogens are dependent on
289 sodium ions for methane formation(36) and the sodium ion concentrations were at a
290 high level (more than 1200 mg/L, as shown in Table 1) in the samples, which
291 provided an appropriate environment for the high abundance of methanogenic
292 archaea.

293 It is unclear how archaea communicated or structurally interacted with their
294 environment. Thus, the methanogens certainly represented the keystone species, but
295 the archaeal diversity beyond the methanogens must not be neglected. *Nitrososphaera*
296 and *Methanosarcina* are the remaining genera found in these samples, and

297 unclassified genera made up less than 0.1%, which verified the low diversity of
298 archaea again. *Nitrososphaera*, which is one of the primary phylotypes of
299 ammonia-oxidizing archaea (AOA)(37), had also been directly linked to active
300 nitrification; it was found that the biotransformation of micropollutants were involved
301 in the co=metabolism of ammonia-oxidizing microorganisms(38, 39).
302 *Methanosarcina* is one of the few methanogens shown to participate in direct
303 interspecies electron transfer (DIET) by directly receiving electrons to reduce CO_2
304 into CH_4(40), and it appeared to be of crucial importance to the anaerobic digestion
305 process(41).

306 (3) Microbial community diversity between two samples

307 Although the syntrophic and competitive relationships between archaea and
308 bacteria remained completely unclear, a consortia of bacterial and archaeal
309 communities played an important role in the degradation of complex organic
310 compounds(36). The ways in which archaea and bacteria define their niche within a
311 complex setting could be revealed by extensive and in-depth studies on microbial
312 community diversities in different environments.

313 The similarity of the pH values, water temperature, ion concentrations and types
314 of organic pollutants between HNC and HNT gave an intimation of the similarity in
315 components in both the archaeal and bacterial communities. The diversity in the
316 concentrations of collectors was the primary reason for the diversity of distributions in
317 the microbial composition. The primary bacterial compositions of both samples
318 consisted of *Desulfomicrobium, Paracoccus, Tindallia, Methanobacterium,*

319 *Methanothrix* and *Nitrososphaera*, which were all reported as alkaliphilic bacteria for
320 biological neutralization(29, 30, 42, 43). The primary archaeal compositions in both
321 samples consisted of (the genera *Methanothrix, Methanobacterium* and
322 *Methanosarcina*) and AOA (genus *Nitrososphaera*), which appear to be part of a key
323 strategy to adapt to a complex environment(32).

324 According to the sample HNC result, the community primarily made up of
325 *Desulfomicrobium, Paracoccus, Tindallia, Methanothrix, Methanobacterium* and
326 *Nitrososphaera* seemed better adapted to the biodegradation of the flotation collectors.
327 Flotation collectors are small molecular organic materials, and they could be degraded
328 by bacteria more easily. The sulfate reduction and ammonia oxidization tasks were
329 performed by *Desulfomicrobium* and *Nitrososphaera*, while other genera played a
330 supporting role.

331 According to the result for the HNT, the community primarily made up of
332 *Paracoccus, Exiguobacterium, Methanothrix* and *Methanobacterium* was considered
333 to be more efficient at biodegrading the flocculant. HPAM, the flocculant in the
334 samples, was a bio-refractory polymer compound with amide groups and a carbon
335 backbone that could be the energy source for microorganisms. In these habitats and
336 with flocculant as a substrate, *Exiguobacterium* produced lactate, acetate and formate,
337 and these products were converted into methane by *Methanothrix* and
338 *Methanobacterium*. *Paracoccus*, the dominant bacterial genus, could grow under
339 aerobic and denitrifying conditions, and it showed great potential at hydrogen sulfide
340 removal from synthetic biogas(44, 45). *Exiguobacterium* was reported to grow

341 through the utilization of molecules containing acyl groups(46). These two bacterial
342 genera supported methanogenesis by methanogens, which was important at the end of
343 the anaerobic digestion chain for biomass conversion.

344 ## 4 Conclusions

345 The archaeal and bacterial communities in recycling effluents from bauxite
346 flotation plant were revealed, and the diversity between the recycling effluent of
347 concentrate and that of tailings was studied. Of the unclassified OTUs at the genus
348 level, almost all fell into the Firmicutes phylum, and they
349 accounted for approximately 40 percent of all the OTUs. Therefore, this recycling
350 effluent was a worthy resource for the isolation of new strains in the Firmicutes
351 phylum. At the genus level, *Paracoccus, Desulfomicrobium, Exiguobacterium,*
352 *Tindallia, Ercella* and *Anoxynatronum* were the primary members of the bacterial
353 community, while *Methanothrix, Methanobacterium, Nitrososphaera* and
354 *Methanosarcina* dominated the archaeal community. The biodegradation of the
355 pollutants in the recycling effluents involved the synergism of bacteria and archaea.
356 Combined with the geochemical properties of recycle effluents, the microbial
357 community containing *Desulfomicrobium, Paracoccus, Tindallia, Methanobacterium,*
358 *Methanothrix* and *Nitrososphaera* was more adept at the biodegradation of flotation
359 collectors, such as hydroximic acid and oleic oil. The microbial community consisting
360 of *Paracoccus, Exiguobacterium, Methanothrix* and *Methanobacterium* was more
361 efficient at the biodegradation of HPAM. The results of this study provided a practical
362 orientation on the biotreatment of recycling effluents from the bauxite flotation

process.

Acknowledge

This research was supported by Funds of the Research and Innovation Project of Graduate Students of Central South University (1053320170205), Fundamental Research Funds for the Central Universities of Central South University (502211704), State Key Laboratory of Advanced Technologies for Comprehensive Utilization of Platinum Metals (SKL-SPM-201809), State Key Laboratory of Applied Microbiology Southern China (SKLAM005-2016), National Natural Science Foundation of China (51320105006, 51504106 and 51871250), Science and Technology Project of Yunnan (2015FB204)

References

1. Zhou X, Yin J, Chen Y, Xia W, Yuan X. Simultaneous removal of sulfur and iron by the seed precipitation of digestion solution for high-sulfur bauxite. Hydrometallurgy. 2018;181:7-15.
2. Xiao-Bin LI, Wang YL, Zhou QS, Tian-Gui QI, Liu GH, Peng ZH, et al. Transformation of hematite in diasporic bauxite during reductive Bayer digestion and recovery of iron. Transactions of Nonferrous Metals Society of China. 2017;27(12):2715-26.
3. Chen XJ. The influence of mineral processing technology of low grade bauxite on the efficiency of Bayer process. World Nonferrous Metals. 2017:37-8.
4. XIA Liu-yin ZH, LIU Guang-yi. Flotation techniques for separation of diaspore from bauxite using Gemini collector and starch depressant. Transactions of Nonferrous Metals Society of China. 2010;20(3):495-501.
5. Chen X, Yao G, Xiong D, Zheng H, Chen J, Yang J, et al. Application research on flocculant for Dressing-Bayer process of alumina production. Light Metals. 2014:21-6.
6. Luo YL, Yang ZH, Xu ZY, Zhou LJ, Zeng GM, Jing H, et al. Effect of trace amounts of polyacrylamide (PAM) on long-term performance of activated sludge. Journal of Hazardous Materials. 2011;189(1):69-75.
7. Lopachin RM, Lehning EJ. Acrylamide-induced distal axon degeneration: a proposed mechanism of action. Neurotoxicology. 1994;15(2):247-59.
8. Chen D, Jin G, Zhang Q, Arowolo AO, Li Y. Water Ecological Function Zoning in Heihe River Basin, Northwest China. Physics & Chemistry of the Earth Parts A/b/c. 2016;96:74-83.
9. Liu X, Lin L, Yu P. Ecological zoning for regional sustainable development using an integrated modeling approach in the Bohai Rim, China. Ecological Modelling. 2016;353:158-66.
10. Briones A, Raskin L. Diversity and dynamics of microbial communities in engineered

396 environments and their implications for process stability. Current Opinion in Biotechnology.
397 2003;14(3):270-6.
398 11. Braga JK, Motteran F, Silva EL, Varesche MBA. Evaluation of bacterial community from
399 anaerobic fluidized bed reactor for the removal of linear alkylbenzene sulfonate from laundry
400 wastewater by 454-pyrosequence. Ecological Engineering. 2015;82:231-40.
401 12. Claesson MJ, O'Sullivan O, Wang Q, Nikkila J, Marchesi JR, Smidt H, et al. Comparative
402 Analysis of Pyrosequencing and a Phylogenetic Microarray for Exploring Microbial Community
403 Structures in the Human Distal Intestine. Plos One. 2009;4(8):e6669.
404 13. Schloss PD, Westcott SL, Ryabin T, Hall JR, Hartmann M, Hollister EB, et al. Introducing
405 mothur: Open-Source, Platform-Independent, Community-Supported Software for Describing and
406 Comparing Microbial Communities. Appl Environ Microb. 2009;75(23):7537-41.
407 14. Antje R, Martha Z, Andreas S, Mandy SN, Rafael S, Alexander G, et al. Characterization of
408 microbial biofilms in a thermophilic biogas system by high-throughput metagenome sequencing. Fems
409 Microbiology Ecology. 2012;79(3):785-99.
410 15. Xie Z, Wang Z, Wang Q, Zhu C, Wu Z. An anaerobic dynamic membrane bioreactor (AnDMBR)
411 for landfill leachate treatment: Performance and microbial community identification. Bioresource
412 Technology. 2014;161(3):29-39.
413 16. Cho JC, Tiedje JM. Bacterial Species Determination from DNA-DNA Hybridization by Using
414 Genome Fragments and DNA Microarrays. Appl Environ Microbiol. 2001;67(8):3677-82.
415 17. Langille MGI, Jesse Z, J Gregory C, Daniel MD, Dan K, Reyes JA, et al. Predictive functional
416 profiling of microbial communities using 16S rRNA marker gene sequences. Nature Biotechnology.
417 2013;31(9):814.
418 18. Zhang L, Loh KC, Lim JW, Zhang J. Bioinformatics analysis of metagenomics data of
419 biogas-producing microbial communities in anaerobic digesters: A review. Renewable and Sustainable
420 Energy Reviews.100:110-26.
421 19. Wang J, Jiang XB, Liu XD, Sun XY, Han WQ, Li JS, et al. Microbial degradation mechanism of
422 pyridine by Paracoccus sp NJUST30 newly isolated from aerobic granules. Chemical Engineering
423 Journal. 2018;344:86-94.
424 20. Nisha KN, Devi V, Varalakshmi P, Ashokkumar B. Biodegradation and utilization of
425 dimethylformamide by biofilm forming Paracoccus sp. strains MKU1 and MKU2. Bioresour Technol.
426 2015;188:9-13.
427 21. Shu C, Cai T, Liu S, Qian Y, Jian H, Chen L, et al. Biodegradation of N-Methylpyrrolidone by
428 Paracoccus sp. NMD-4 and its degradation pathway. International Biodeterioration & Biodegradation.
429 2014;93:70-7.
430 22. Zhou J. Biological removal of nitrate and ammonium under aerobic atmosphere by Paracoccus
431 versutus LYM. Bioresource Technology. 2013;148(7):144-8.
432 23. Song J, Chen L, Chen H, Sheng F, Xing D, Ling L, et al. Characterization and high-throughput
433 sequencing of a trichlorophenol-dechlorinating microbial community acclimated from sewage sludge.
434 Journal of Cleaner Production. 2018:S0959652618317116-.
435 24. Xin-Yang YU, Wang HL, Wang QQ, Feng B, Zhong H. Flotation of low-grade bauxite using
436 organosilicon cationic collector and starch depressant. Transactions of Nonferrous Metals Society of
437 China. 2016;26(4):1112-7.
438 25. Kulshreshtha NM, Kumar A, Dhall P, Gupta S, Bisht G, Pasha S, et al. Neutralization of alkaline
439 industrial wastewaters using ☆. International Biodeterioration & Biodegradation. 2010;64(3):191-6.

26. Bharti N, Yadav D, Barnawal D, Maji D, Kalra A. Exiguobacterium oxidotolerans, a halotolerant plant growth promoting rhizobacteria, improves yield and content of secondary metabolites in Bacopa monnieri (L.) Pennell under primary and secondary salt stress. World J Microb Biot. 2013;29(2):379-87.

27. Selvakumar G, ., Kundu S, ., Piyush J, Sehar N, Gupta AD, Gupta HS. Growth promotion of wheat seedlings by Exiguobacterium acetylicum 1P (MTCC 8707) a cold tolerant bacterial strain from the Uttarakhand Himalayas. Indian Journal of Microbiology. 2010;50(1):50-6.

28. Yeong OS, Su HN, Shruti S, Sung-Min K, Ilsong L, Hoomin L, et al. Multi-stress radioactive-tolerant Exiguobacterium acetylicum CR1 and its applicability to environmental cesium uptake bioremediation. Journal of Cleaner Production. 2018;205:281-90.

29. Sousa JAB, Plugge CM, Stams AJM, Bijmans MFM. Sulfate reduction in a hydrogen fed bioreactor operated at haloalkaline conditions. Water Research. 2015;68:67-76.

30. Ryzhmanova Y, Oshurkova V, Troshina O, Abashina T, Ariskina E, Avtukh A, et al. Anoxynatronum buryatiense sp. nov., an anaerobic alkaliphilic bacterium from a low mineralization soda lake in Buryatia, Russia. International Journal of Systematic & Evolutionary Microbiology. 2017;67(11):4704-9.

31. Gelder AH, Van, Sousa DZ, Rijpstra WIC, Damsté JSS, Stams AJM, Irene SA. Ercella succinigenes gen. nov., sp. nov., an anaerobic succinate-producing bacterium. Int J Syst Evol Microbiol. 2014;64(Pt 7):2449-54.

32. Moissl-Eichinger C, Pausan M, Taffner J, Berg G, Bang C, Schmitz RA. Archaea Are Interactive Components of Complex Microbiomes. Trends in Microbiology. 2018;26(1):70-85.

33. Sirohi SK, Pandey N, Singh B, Puniya AK. Rumen methanogens: a review. Indian Journal of Microbiology. 2010;50(3):253-62.

34. Do TM, Stuckey DC, Oh S. Effect of ciprofloxacin on methane production and anaerobic microbial community. Bioresource Technology. 2018;261:240-8.

35. Rui JP, Qiu QF, Lu YH. Syntrophic acetate oxidation under thermophilic methanogenic condition in Chinese paddy field soil. Fems Microbiology Ecology. 2011;77(2):264-73.

36. Gottschalk G, Thauer RK. The Na + -translocating methyltransferase complex from methanogenic archaea. BBA - Bioenergetics. 2001;1505(1):28-36.

37. Gao JF, Luo X, Wu GX, Li T, Peng YZ. Quantitative analyses of the composition and abundance of ammonia-oxidizing archaea and ammonia-oxidizing bacteria in eight full-scale biological wastewater treatment plants. Bioresource Technology. 2013;138(6):285-96.

38. Yan Y, Ma M, Xiang L, Ma W, Miao L, Yan L. Effect of biochar on anaerobic degradation of pentabromodiphenyl ether (BDE-99) by archaea during natural groundwater recharge with treated municipal wastewater. International Biodeterioration & Biodegradation. 2017;124:119-27.

39. Chen H, Yue Y, Jin W, Xu Z, Wang Q, Gao SH, et al. Enrichment and characteristics of ammonia-oxidizing archaea in wastewater treatment process. Chemical Engineering Journal. 2017;323:465-72.

40. Stuart AG, Sharples PM, Eyre JA, Aynsley-Green A, Heaviside DW. Direct interspecies electron transfer between Geobacter metallireducens and Methanosarcina barkeri. Applied & Environmental Microbiology. 2014;80(15):4599.

41. Vrieze JD, Hennebel T, Boon N, Verstraete W. Methanosarcina : The rediscovered methanogen for heavy duty biomethanation. Bioresource Technology. 2012;112(5):1-9.

42. Peng ZX, Hui-Jun HE, Yang CP, Zeng GM, Wen S, Yan Z, et al. Biological treatment of

484 wastewater with high concentrations of zinc and sulfate ions from zinc pyrithione synthesis.
485 Transactions of Nonferrous Metals Society of China. 2017;27(11):2481-91.
486 43. Kim J, Kim H, Lee C. Ulva biomass as a co-substrate for stable anaerobic digestion of spent
487 coffee grounds in continuous mode. Bioresource Technology. 2017;241:1182-90.
488 44. Vikromvarasiri N, Boonyawanich S, Pisutpaisal N. Optimizing Sulfur Oxidizing Performance of
489 Paracoccus Pantotrophus Isolated from Leather Industry Wastewater ☆ . Energy Procedia.
490 2015;79:629-33.
491 45. Vikromvarasiri N, Juntranapaporn J, Pisutpaisal N. Performance of Paracoccus pantotrophus for
492 H 2 S removal in biotrickling filter. International Journal of Hydrogen Energy. 2017;42(45):27820-5.
493 46. Shamshuddin Z, Kirse C, Briesen H, Doble M. Mathematical modelling of AHL production in
494 Exiguobacterium MPO strain. Biochem Eng J. 2018;138:54-62.

495

Fig 1 Flow chart of desilication process and sample collection

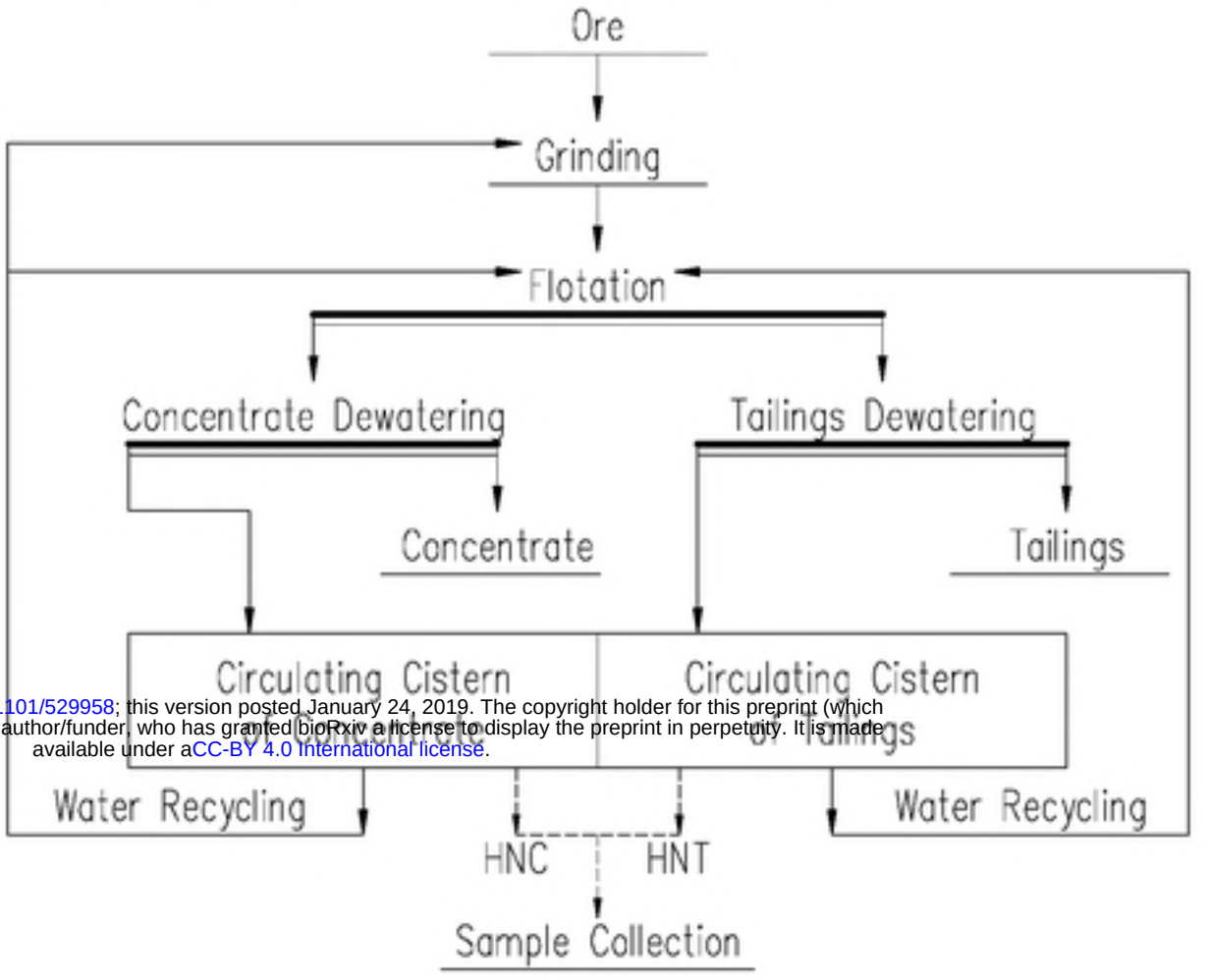

Figure 1

Fig 2 Curves from the Shannon rarefaction analysis (a-bacteria, b-archaea)

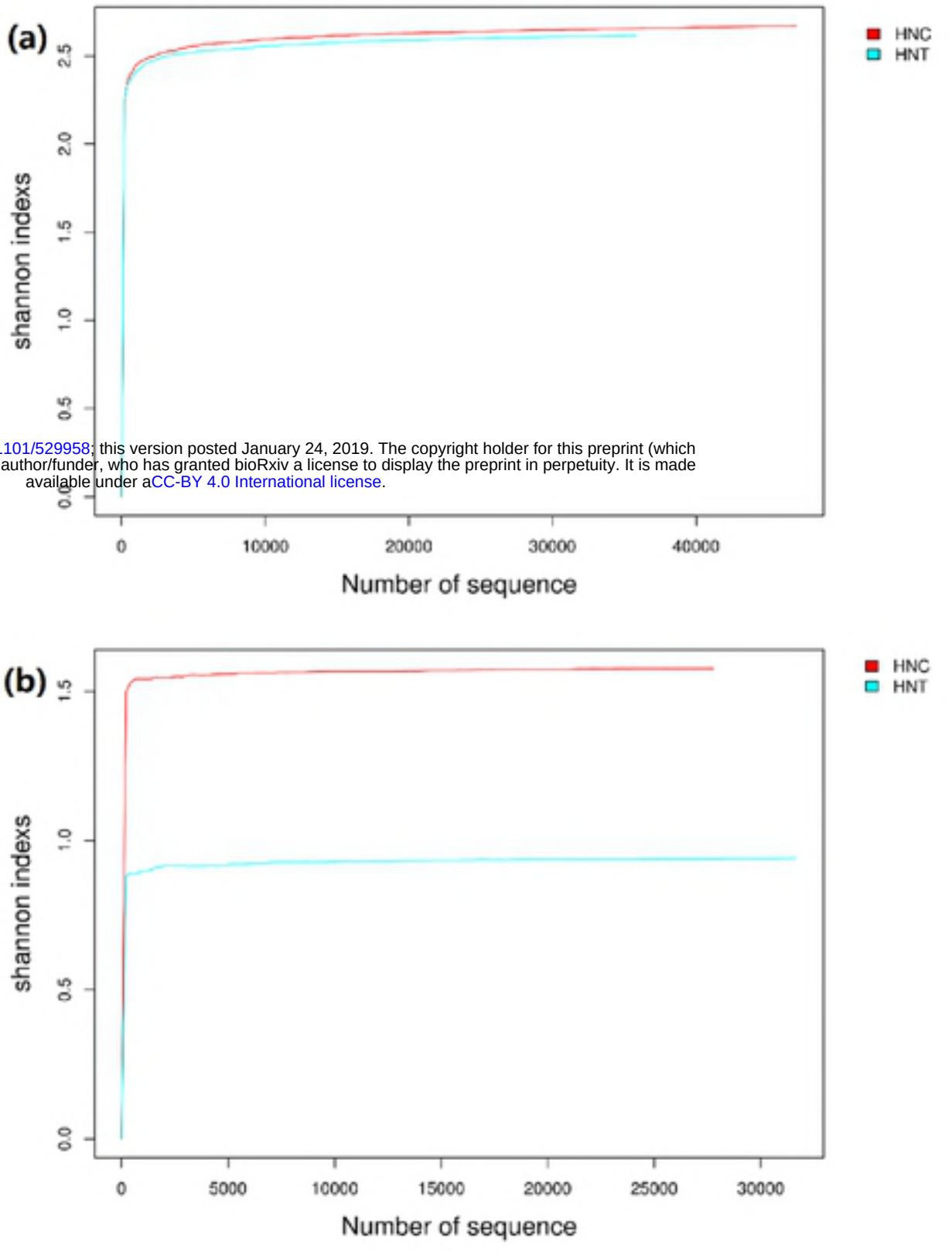

Figure 2

Fig 3 Rank abundance curves based on OTU ranks (a-bacteria, b-archaea)

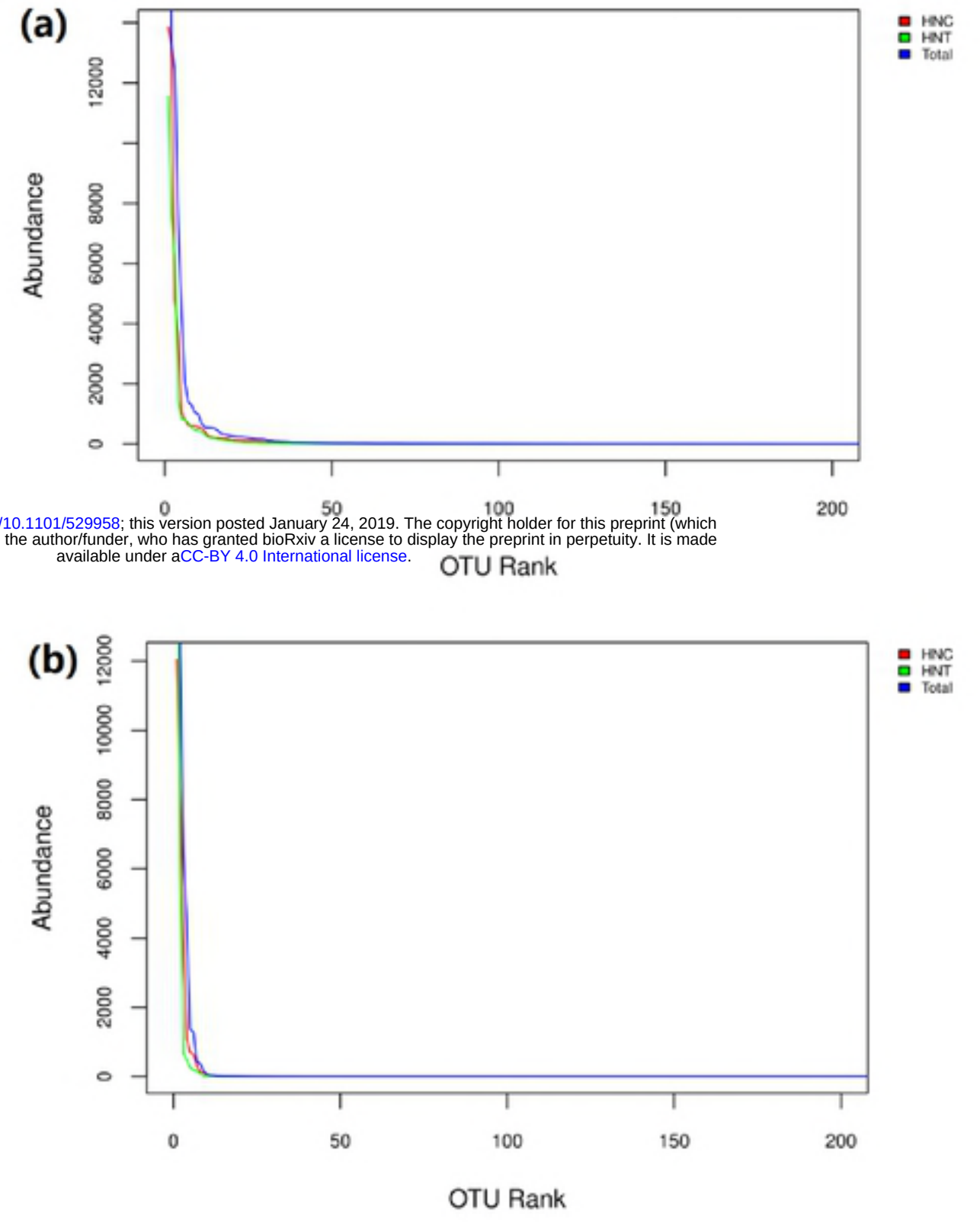

Figure 3

Fig. 4 Similarity and overlap analysis of OTUs by Venn diagram

(a-bacteria, b-archaea)

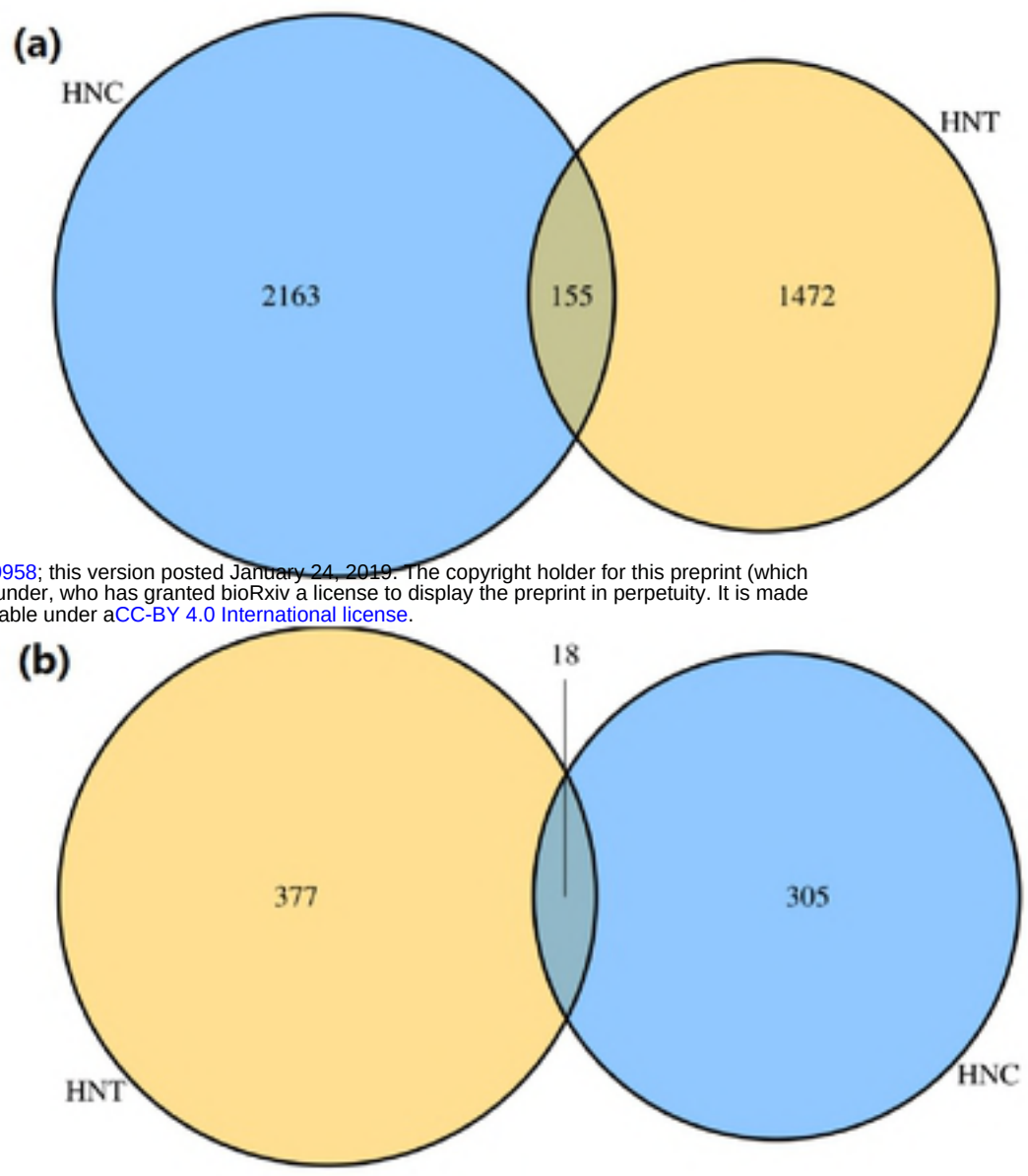

Figure 4

Fig 5 Taxonomic distribution of bacterial OTU abundance at the phylum level

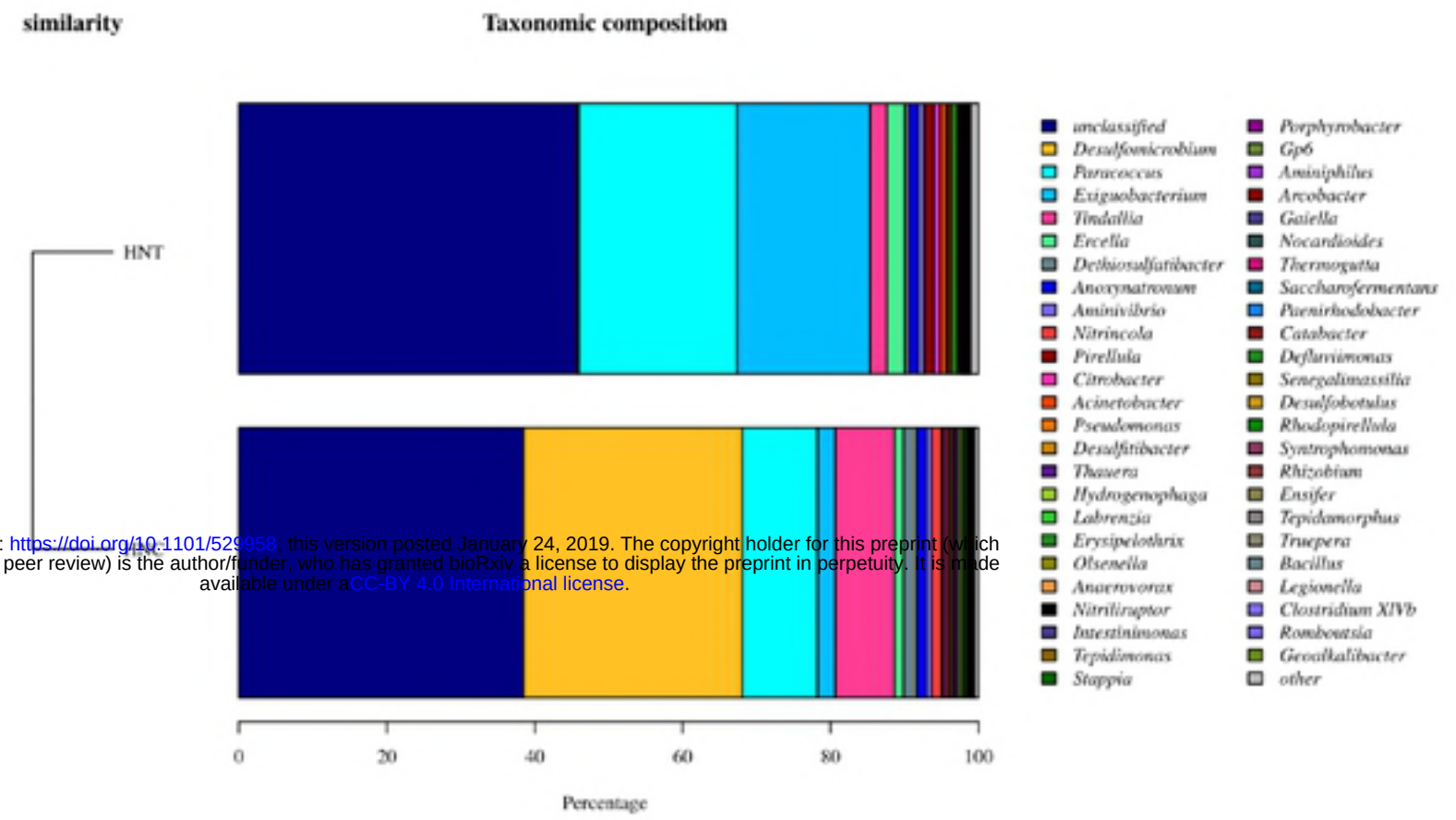

Figure 5

Fig 6 Phylogenetic compositions and community structures of bacteria

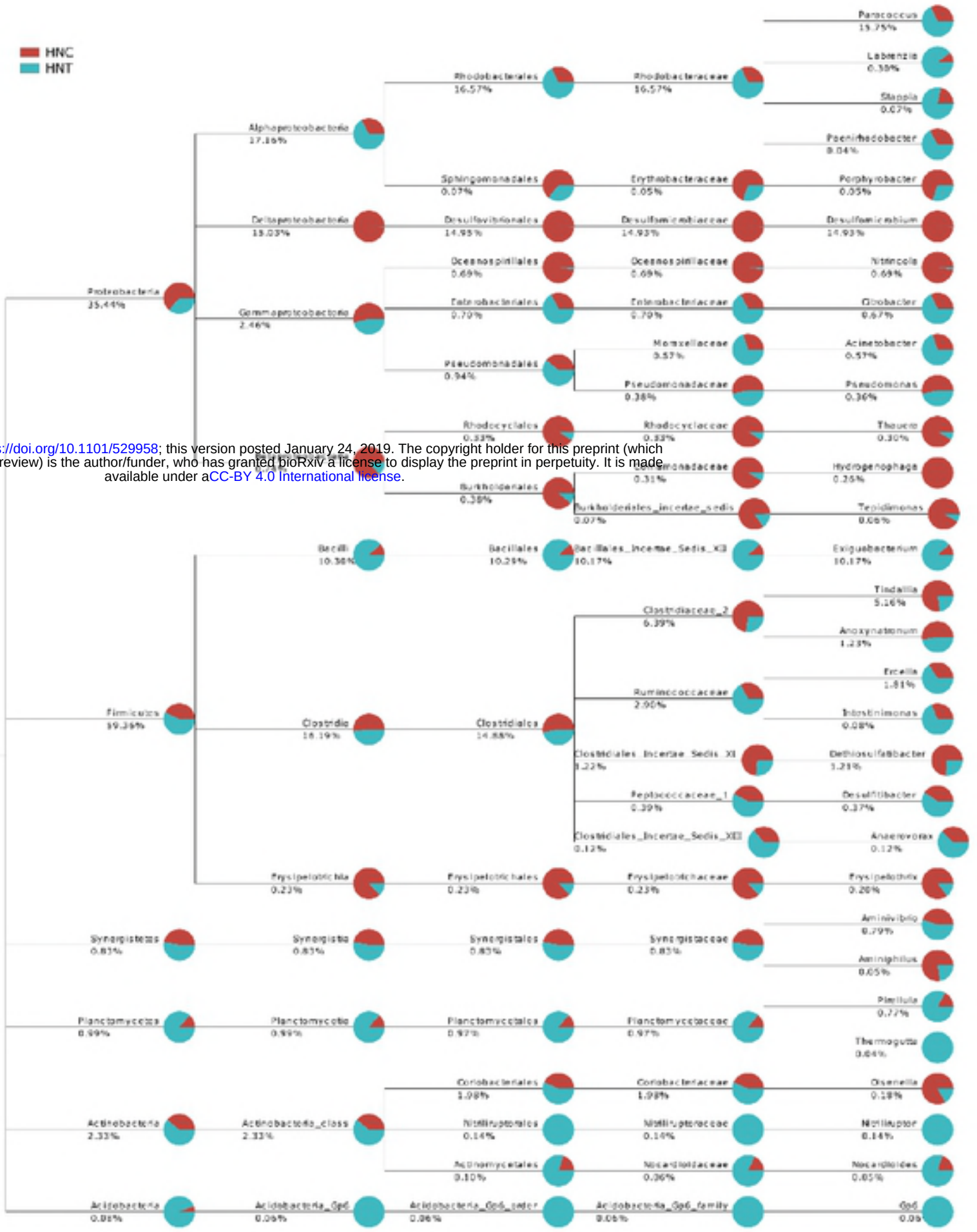

Figure 6

Fig 7 Taxonomic distribution of archaeal OTU abundance at the phylum level

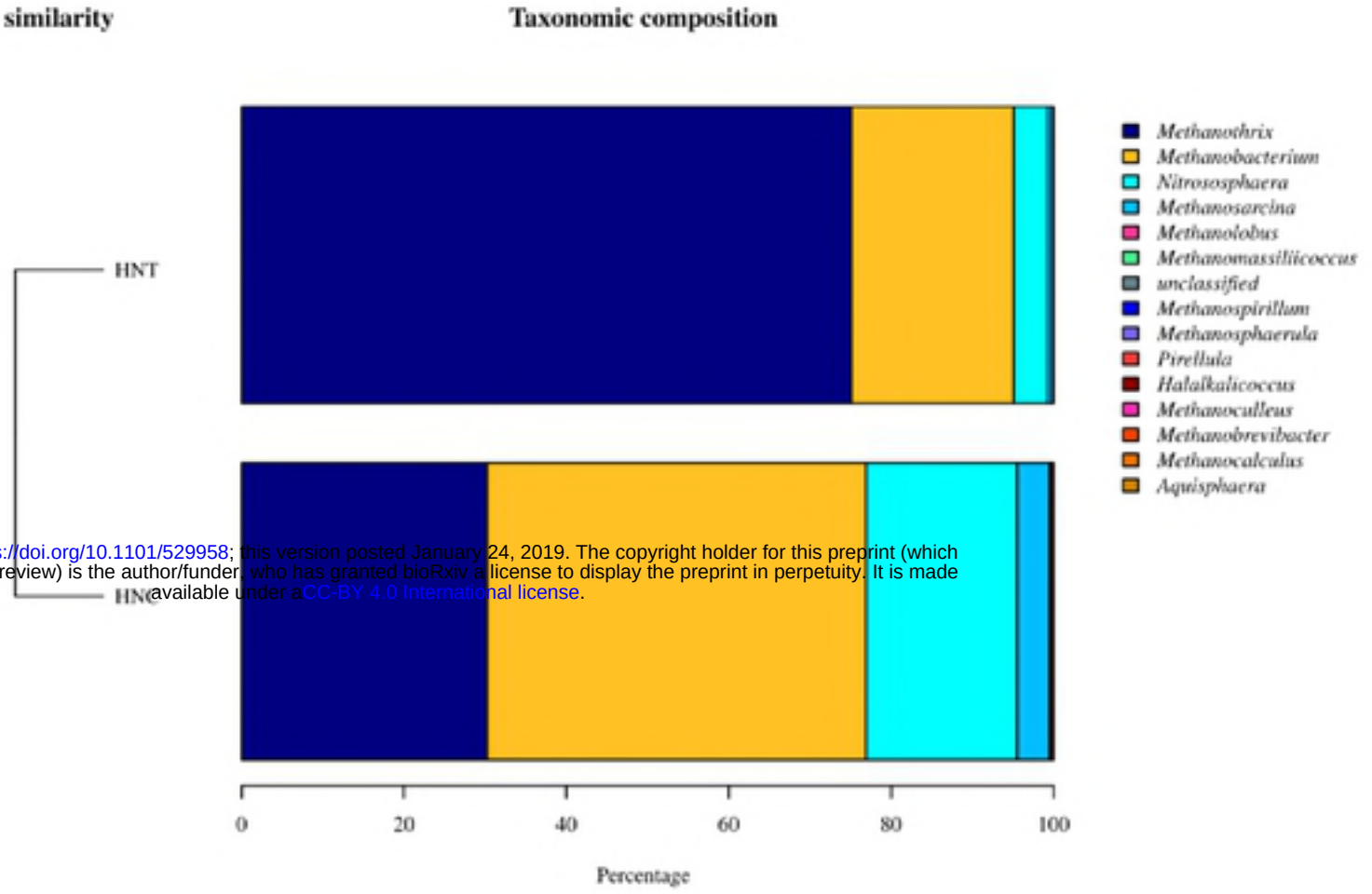

Figure 7

Fig 8 Phylogenetic compositions and community structures of archaea

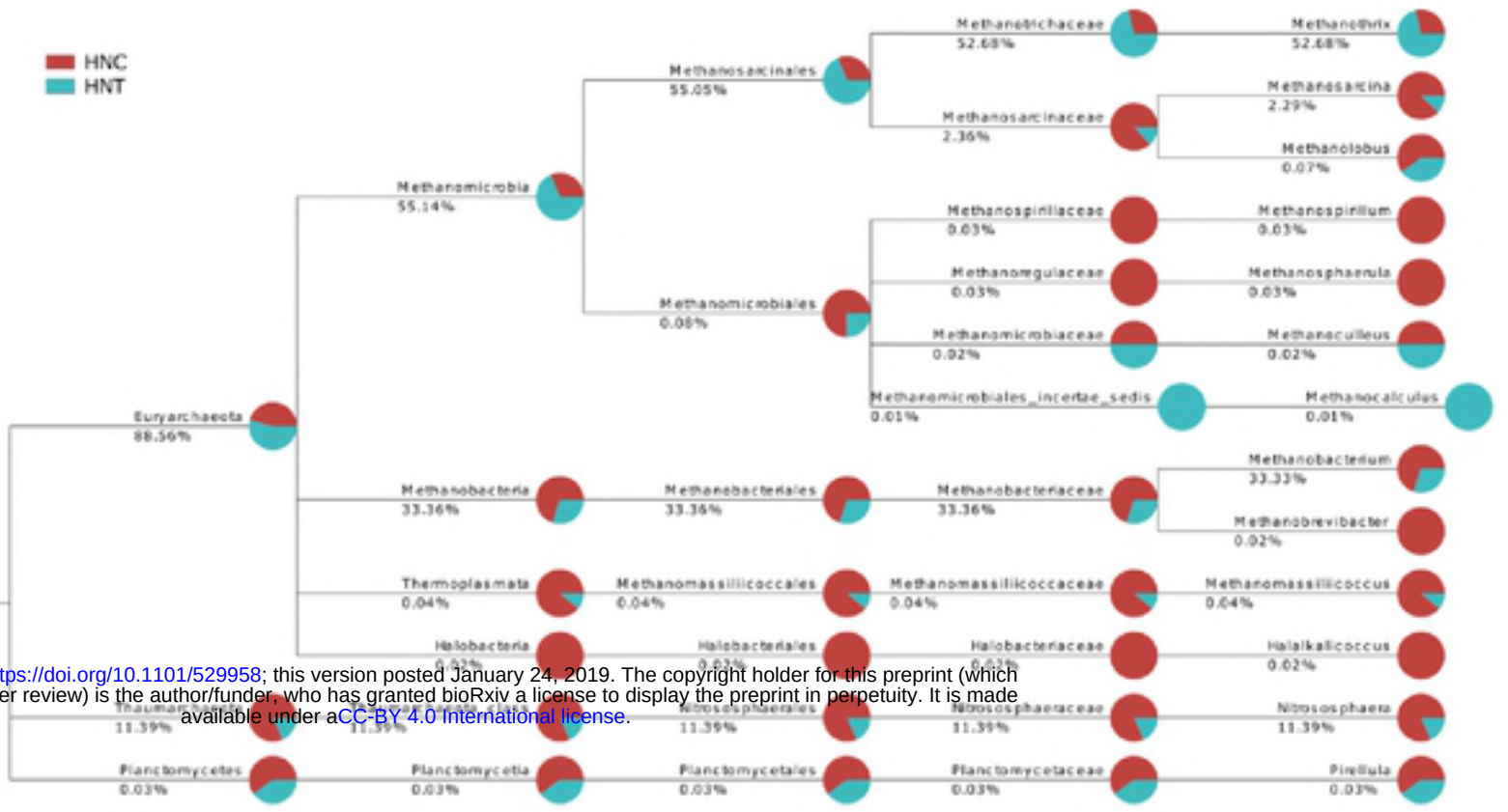

Figure 8